First results of the spectral characterisation of a salt flat in Europe: the Sal 'e Porcus salty pond

Maria Teresa Melis[1], Massimo Musacchio[2], Marco Casu[1,3], Claudia Collu[1,3], Mariana Correa[4], Lorenzo Sedda[1], Malvina Silvestri[2], Fabrizia Buongiorno[2], Federico Rabuffi[2], Stefano Andreucci[1], Jan Kanuk[5], Michal Gallay[5], Katarina Onacillova[5], Jan Sasak[5], Stefano Naitza[1], Giovanni Fantini[1], Francesco Dessì[1], Salvatore Noli[1]

[1] Department of Chemical and Geological Sciences, Cittadella Universitaria (Blocco A)-S.S. 554 Bivio per Sestu, 09042 Monserrato (CA), Italy - titimelis@unica.it
[2] Istituto Nazionale di Geofisica e Vulcanologia, Osservatorio Nazionale Terremoti, Via di Vigna Murata 605, 00143 Roma, Italy- massimo.musacchio@ingv.it
[3] Department of Earth Sciences (DES), La Sapienza Università di Roma—Piazzale Aldo Moro 5, 00185 Roma, Italy
[4] Universidad Nacional de Río Cuarto Ruta Nac. 36 - KM. 601 - Río Cuarto - Córdoba - Argentina– marianalucia.correa@gmail.com
[5] Institute of Geography, Faculty of Science, Pavol Jozef Šafárik University in Košice, Slovakia - jan.kanuk@upjs.sk

Keywords: Hyperspectral data, Spectral Library, Evaporites, PRISMA, Salt Flat, LiDAR.

Abstract

Sal ‘e Porcus is the largest natural salt flat in Europe, located in Sardinia (Italy) in the southwest region of the Mediterranean area. It spans over an area of more than 3.3 square kilometers. Its homogeneity and size characteristics make it a potentially suitable spot for use as a satellite sensor calibration/validation site. For this purpose, a campaign of spectral, mineralogical and LiDAR data acquisition has been organized in the framework of a dedicated International Remote Sensing Summer School in 2023. Furthermore, the study of this site has been funded by the Italian Spatial Agency through the Project: System for the “*COnsOlidation of L2 products from the PRISMA-SG mission (COOL)*”.
New orbiting hyperspectral sensors such as ASI-PRISMA and EnMAP DLR and near future continuity missions (ASI-PRISMA SG, ESA CHIME) request ground reflectance spectra to rely on the remote sensed data. In this study, the first results of the study of the spectral and LiDAR data acquired on the site are described and discussed, focusing on two main outputs: i) the first release of the spectral library of the minerals of the salt flat; ii) the morphological setting of the surface.
The collection of the spectra has been coupled with sediment samples for mineralogical characterization. During these campaigns, UAV-based LiDAR data were acquired. First results show that the topography of the surface changes from west to east, giving the idea of a geological control of this flat area. Moreover, first results of the spectral characterization of this surface using field, UAV and satellite data are discussed.

1. Introduction

The increasing interest in hyperspectral data acquired from satellite sensors and from UAVs for earth observation purposes has driven the authors to propose the creation of spectral libraries for calibration/validation (CAL/VAL) studies. One of the main issues using or proposing new sensors is the testing of the performance of these instruments on specific land sites with known physical characteristics.
In Sardinia, a site has been recognised as potential candidate for CAL/VAL of hyperspectral sensors. A large flat area composed by an evaporite crust during the summer season and recognised as a protected area seems to respond to the requested characteristics to be an aspirant site. Its homogeneity and size characteristics make it a potentially suitable spot for use as a satellite sensor CAL/VAL site.
The preliminary positive results already obtained using data from ASI-PRISMA and DLR-EnMAP, to candidate the site of Sal ‘e Porcus pond for CAL/VAL purposes, can be improved with new physiographic and spectral data. Moreover, near future continuity missions (ASI-PRISMA SG, ESA CHIME) require ground reflectance spectra to validate on the remote sensed data (Musacchio et al., 2024).
For this purpose, a campaign of spectral and morphological detailed data acquisition has been organized in the framework of a dedicated International Remote Sensing Summer School in 2023. Furthermore, the study of this site has been funded by the Italian Spatial Agency through the Project: System for the COnsOlidation of L2 products from the PRISMA-SG mission (COOL).
In this study, the first results of the analyses of spectral and LiDAR data acquired on the site are described and discussed, focusing on two main outputs: i) the first release of the spectral library of the salt flat minerals; ii) the morphological setting of the surface.
The primary role of this spectral library will be to provide auxiliary information for the calibration of hyperspectral data acquired from aircraft and from spacecraft. As well known, spectroscopy comprehends several techniques and methodologies aimed to investigate the nature of materials, analysing their emitted or/and reflected electromagnetic radiation across different wavelengths. The characteristics of the resulting spectra, produced when materials interact with or emit electromagnetic radiation, including distinct adsorption features, are directly determined by the chemical, physical or structural properties of investigated material. Therefore, in this study, the radiometric information collected from field measures have been compared with laboratory sample analysis from the X-Ray Diffraction analyses (XRD) to detect their mineralogical composition.
In order to analyse the morphology of a surface, several techniques using very high-resolution satellite optical data are described (Melis et al, 2021). Furthermore, LiDAR data allow to create the digital surface/elevation model (DSM, DEM) with a very high spatial resolution. Moreover, this sensor mounted on a UAV can perform the requested elevation accuracy. The UAV remote sensing allows for custom data collection matching the

user needs and environmental settings (Kaňuk et al. 2018). Many areas in Europe are covered by national lidar data, but this is not the case of the Sal’e Porcus lake. The low flight altitude allows for acquisition in high spatial resolution which the national data typically do not provide. To provide sufficient evidence of spectral uniformity of the salt pan and its relevance for calibration of the satellite sensors, UAV-based hyperspectral imaging provides means for characterising the surface material over larger areas than with a field spectrometer and in a high spatial detail.

2. The site

2.1 Geographic location

Sal ‘e Porcus pond is the largest natural salt flat in Europe and it is located in the West of Sardinian region. (Italy). It spans over an area of more than 3.3 square kilometres (Figure 1).

Figure 1. Map showing the location of the Sal 'e Porcus salt pond in Sardinia, Italy. This site has been identified as a potential candidate for hyperspectral sensor calibration and validation studies.

Considering the lack of drainage outlets, the system of cycling flooding and drying is not well known. The basin, with a maximum depth of 1 metre and an average depth of 40 cm, is characterised by the absence of tributaries and emissaries, indeed it represents an independent basin from the other pond areas present in the area.

During the summer period, the strong evaporation causes the fully dry out of the pond, presenting itself as a large expanse of salt. To determine the annual variation of humidity, a multi-temporal analysis of Sentinel-2 images has been performed. This preliminary study aims to better understand the evolution of such natural phenomenon and to organize the field campaign for spectral measurements.

2.2 Geological setting

The studied salty pond is located on the northern tip of the Sinis Peninsula which is dominated by several geological formations spanning from upper Oligocene to Holocene. In this study, a new preliminary geological sketch map has been developed based on fieldwork data (campaign conducted over several days between December 2023 and March 2024) and previous studies. All formation contacts have been refined using 1-meter resolution existing LiDAR data to achieve greater accuracy and detail (Figure 2).

The most ancient formations are the Atzori Andesites which lay directly on the Palaeozoic basement. The Ussana Formation lays on top of these volcanic rocks and is composed of alluvial sandstones and conglomerates belonging to the first sedimentary cycle. The Villagreca Limestones, composed of reef environment limestones and calcarenites, are part of the same sedimentary cycle, originating during the Aquitanian transgression. Following these are the deposits of the third sedimentary cycle, known as the "Messinian" sequence, which includes the Capo San Marco Formation, the Laminated Limestones of Sinis, and the Torre del Sevo Limestones. The Capo San Marco Formation comprises argillites, marls, and calcarenites containing bivalve fossils. The depositional environment is considered sublittoral, gradually transitioning to a lagoon environment. The Laminated Limestones of Sinis include marls and micritic limestones with seismic shock structures, where the only fossil content consists of foraminifera and small gastropods in the basal part. This formation environment is a carbonate platform. The Torre del Sevo Limestones, on the other hand, consist of brecciated limestones and dolomitic limestones forming a gravitational collapse breccia in an evaporitic environment.

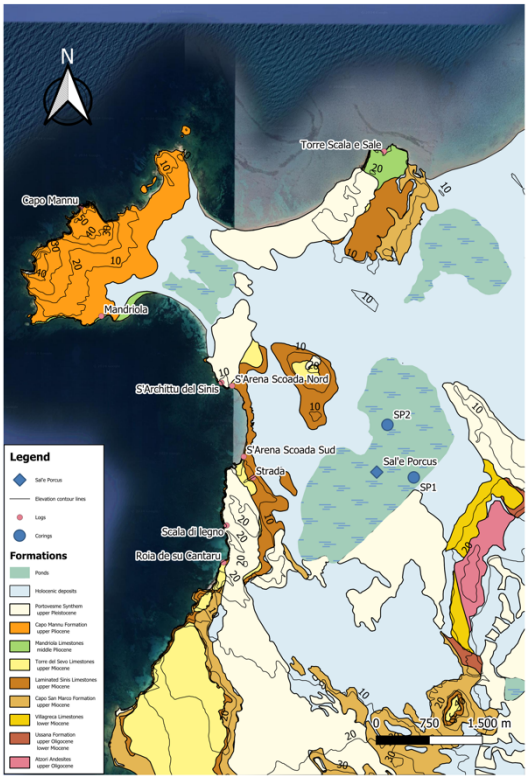

Figure 2. Geological sketch map of the area of Sal ‘e Porcus.

The Pliocene is represented in the northwest by the Mandriola Limestones and the Capo Mannu Formation. The Mandriola Limestones are calcareous rocks containing foraminifera, gastropods, bivalves, shark teeth, and whale bones, with sedimentary structures indicative of a beach environment. The Capo Mannu Formation develops in seven distinct dune complexes separated by red paleo-soils and is attributed to a transitional continental-marine environment (Figure 2).
Sal’e Pocus salty pond is a depression, and its origin is not fully understood. It is particularly important to comprehend its geological and geomorphological dynamics connected with tectonic stress and climatic fluctuations to understand the present water fluctuations and chemical characteristics.

To improve the recent geological evolution of the pond, two three meters depth sediment cores have been drilled (SP1 and SP2 in Figure 2). The first analyses of these sediments show very few evidence of organic remains and an alternation of fine sediment and sand.

3. Methods

3.1 Field Spectroscopy measurements and sampling

Spectroscopic field measurements were made using a Malvern Panalytical portable spectroradiometer ASD Fieldspec3 with the 25° FOV bare fiber. This instrument collects spectra across VIS/SWIR (0.35–2.5 µm) wavelength ranges. The campaign has been carried out the 4th of July 2023 with optimal cloud conditions. The acquisitions focused on the noth-western part of the site (Figure 3), averaging 10 measurements per point. The measurements were converted into reflectance using a tripod mounted white reference panel.
The samples collected on the field were measured in the laboratory through the X-Ray Diffraction analyses (XRD) to detect their mineralogical composition. Mineralogical analysis (XRD) is a useful technique for investigating the crystallographic structure of a solid compound.

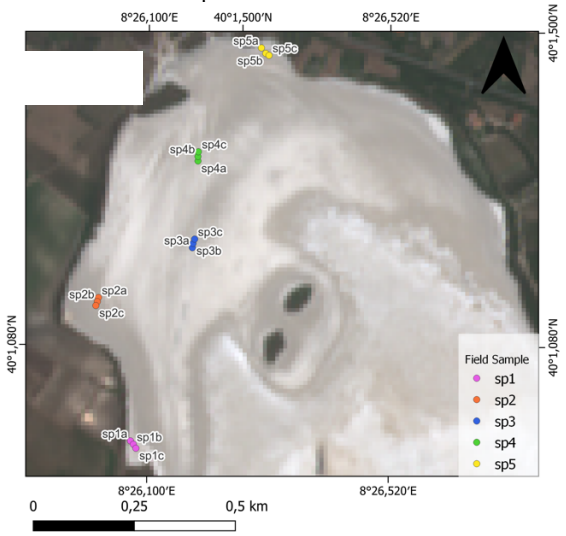

Figure 3. Field- Spectral sampling and acquisition points locations.

3.2 Laboratory spectroscopic measurements

Laboratory-based spectroscopic measurements were conducted using an ASD Fieldspec3 with a mounted 10mm contact probe. Fifteen desiccated and pulverized samples from the 04/07/2023 campaign were collected. Reflectance measurements were conducted with white reference measurements taken before each sample to ensure high accuracy. For each sample, a minimum of three measurements were taken, averaged, and then stored in the SPP library.

3.3 PRISMA Hyperspectral analysis

A PRISMA L2D, orthorectified and atmospherically corrected (R. Guarini et al., 2018), product has been used for the preliminary Hyperspectral analysis on the site. The pre-processing steps consisted in bad-bands and noise removal, the last one using ENVI Minimum Noise Fraction procedure (Figure 4). The ENVI built-in USGS (Kokaly, R.F et, al., 2017) spectral library (minerals_beckam3375) has been resampled and used for a first classification of the site. Finally, the continuum removed (Clark et al., 1987) image and spectral library were used for a Spectral Angle Mapper-based classification in the 2100-2400 nm spectral range.

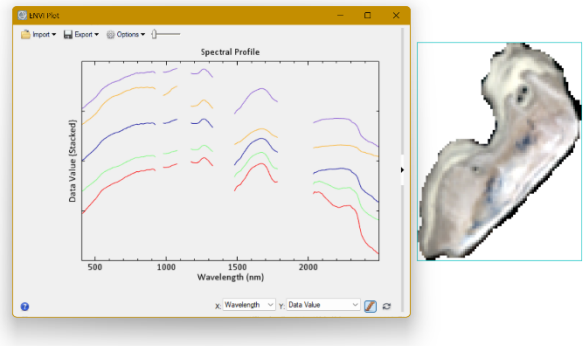

Figure 4. PRISMA L2D pre-processed image of the salty pond, showing different horizons.

3.4 UAV acquisitions

During these campaigns, UAV-based LiDAR and hyperspectral imaging data (HS) were acquired to extract a very high-resolution Digital Terrain Model (DTM) and map the large-scale spectral properties of northern part of the lake. Both kinds of UAV missions were performed in east-west flight direction. Airborne LiDAR point cloud was collected by a VUX-1 scanner manufactured by RIEGL mounted on a custom modification of DJI AGRAS T30 multicopter. The same UAV platform was used to collect hyperspectral data with an AISA Kesttrel 10 push-broom camera manufactured by SPECIM. The same UAV platform was used to collect hyperspectral data with an AISA Kesttrel 10 push-broom camera (spectral range 380-1000 nm) manufactured by SPECIM. The meteorological conditions during both UAV missions flights were stable, characterized by clear skies and moderate wind gusts, with an air temperature of 43°C. The position and orientation of the lidar and hyperspectral sensors are precisely monitored by dual GNSS antennas and an embedded INS unit xNAV550 manufactured by OXTS. The sensors and flight line processing are described in more detail in Kaňuk et al. (2018). Thanks to the flight line post processing with differential corrections from a custom GNSS reference station placed in the field the absolute accuracy of the final data within the WGS84, UTM32N projection system reached standard deviation of few centimetres.

3.5 Multi-temporal analysis

407 Sentinel-2 multispectral images were selected, covering the period from March 2017 to December 2022, and pre-processed to mask clouds and shadows using Sentinel Hub’s Cloud Probability map. Pixels with a probability higher than 20% were masked. From this pre-processed dataset the Normalized Difference Water Index (NDWI) (1) time-series has been extracted, aiming to map over time the spatial distribution of water surfaces over the Sal’e Porcus pond, and thus, determine the periods of total drying.

$$NDWI = \frac{GREEN - SWIR}{GREEN + SWIR} \quad (1)$$

where *GREEN = reflectance at Sentinel-2 B2 band (Central wavelength: 560.0 nm*
SWIR = reflectance at Sentinel-2 B11 band (Central wavelength: 1613.7 nm)

4. Results and discussion

4.1 Spectral analysis

A first step toward the building of a comprehensive spectral library of Sale’e Porcus salty Pond has been made, collecting 15 high quality spectra both in field and laboratory conditions. (Figure 5). Coupled XRD (Figure 6) and future XRF measurements on the current and on future campaigns samples will ensure the completeness of the data stored in the spectral library.

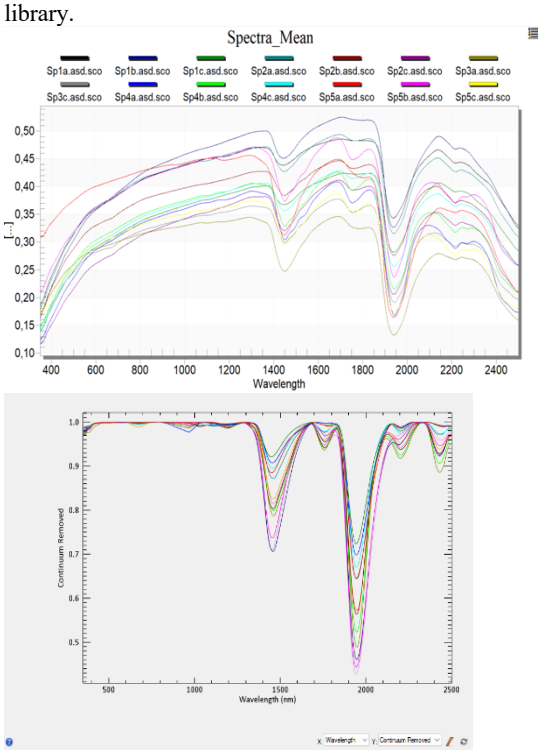

Figure 5. Laboratory-based measurements carried with a 10mm contact probe mounted on ASD Fieldspec3. Mean spectra on the top, continuum removed on the bottom.

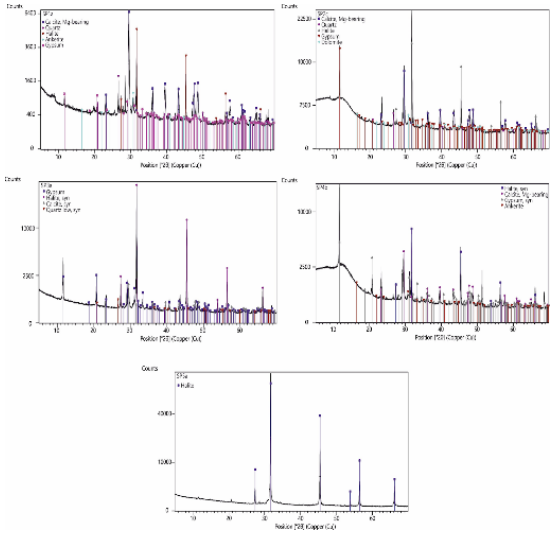

Figure 6. Some of the XRD results from 04/07/2023 field sampling.

Gypsum, Polyhalite and Epsomite emerged from the first classification analysis (Figure 7). This partially agrees with the XRD measurements as Gypsum and halite were present nearly in all the samples. Unexpectedly, despite his presence in nearly all fifteen samples resulting from XRD, calcite main absorption feature at 2330-2335 nm (Clark et, al., 1990) was not observed in the PRISMA image.

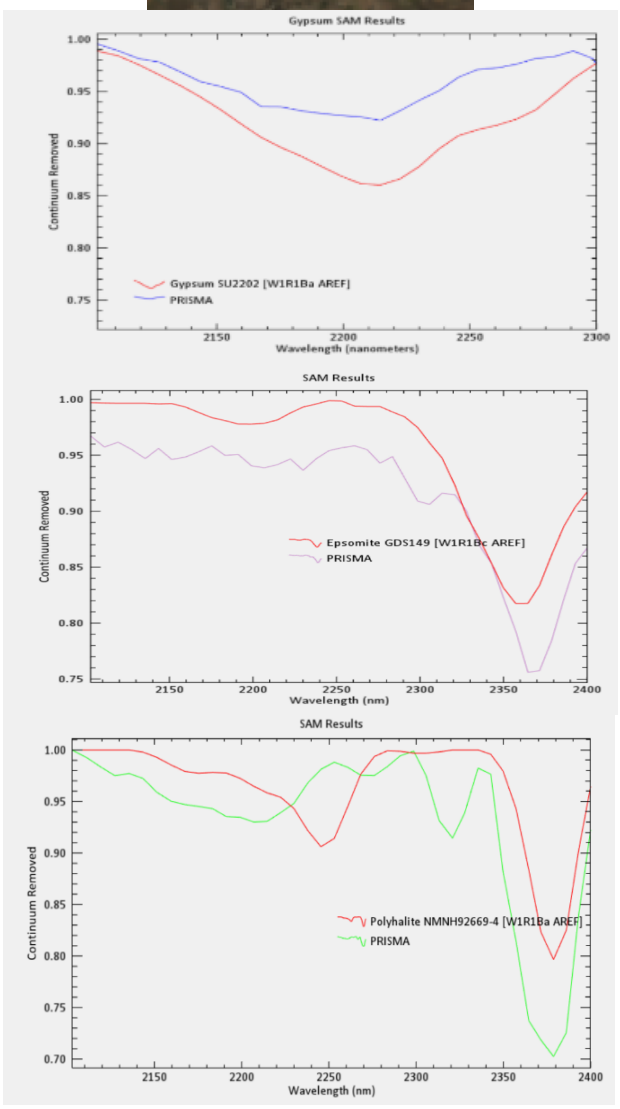

Figure 7. First SAM classification results using PRISMA L2D Hyperspectral data. Resampled minerals_beckam_3375 USGS spectral library was used as reference spectra.

4.2 UAV Lidar data

The lidar data was collected on 19 July 2023 during multiple flights summing for 40 minutes during noon. The flight altitude was 80 m above ground level and flight speed 7 m/s, with a 40 m spacing between flight lines. We used 550 kHz pulse repetition rate at 90 degrees nadir field of view resulting in and average point density of 700 points/m2.collection resulted in 11 flight strips which were first geometrically aligned using the RiProcess software by RIEGL and subsequently improved by the BayesStripAlign 2.1 tool software. The final strip alignment resulted in standard deviation of 0.004 m (Figure 8).

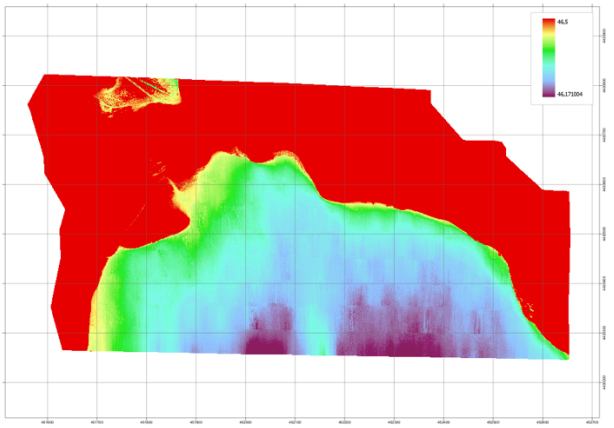

Figure 8. Lidar based DTM of the northern part of Sal e Porcus salty pond. The coulor scheme is adjusted to the elevation range of the lake 46.5 - 46.20 m from yellow to dark blue.

4.3 UAV Hyperspectral data

The HS data collection comprised multiple flights summing for 120 minutes on 17 and 20 July 2023 during noon. The flight altitude was 80 meters and flying speed 5 m/s. The solar azimuth ranged from approximately 160 to 230 degrees and the solar elevation angle from 69 to 63 degrees during both dates. 9 flight strips were acquired with 40 degrees nadir field of view. The raw HS data were radiometrically calibrated and georectified in CaliGeo software pro by SPECIM resulting in 10 cm pixel size (Figure 9). Five radiometric targets differing in reflectance were placed on the salt pan to radiometrically correct the HS data in ENVI software using the empirical line correction method (ELC). The target reflectance was recorded in the field by the ASD FieldSpec (Figure 10).

Figure 9. Line 1-6 acquired 20 July and lines 7,8,9 on 18 July 2023 raw data processed in CaligeoPro, by Specim.
DN processed as raw data – dark current, then into radiance
Georeferenced AISA data file radiometrically corrected to radiance (mW/cm^2*str*um)*1000.00

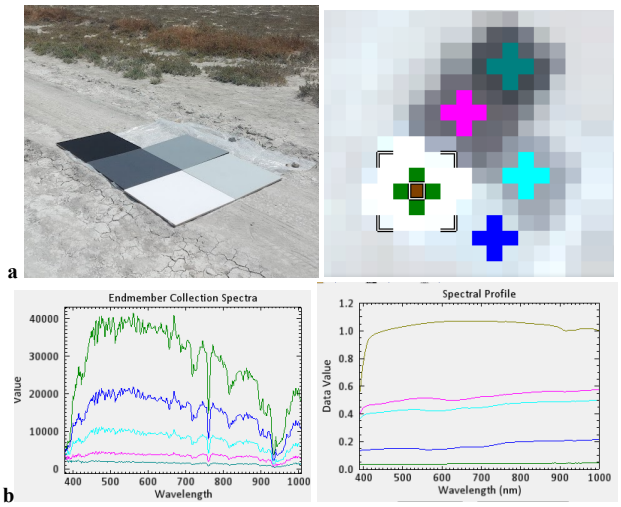

Figure 10. **a)** Radiometric targets used for the correction: on the left the targets in the field, and on the right, the targets as they appear in the UAV hyperspectral image; **b)** the two graphs represent the radiance of the radiometric targets, scale factor 1000, (left) and the ASD field measured reflectance of the radiometric targets (right)

This reflectance values were used in ELC to calculate reflectance of lines 1-6 from radiance data. These lines were chosen as they were acquired in the meantime of the flight. The resulting spectral signature extracted from the processed image of two points (salt surface and vegetation cover) can be seen in Figure 11. These values can be considered a very good preliminary radiometric result of the behaviour of the analysed surfaces.

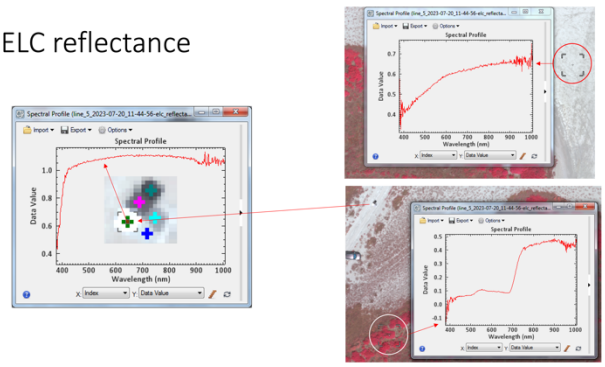

Figure 11. ELC reflectance of the different targets: white panel (left), salt pond surface (up-right), and vegetation (bottom-right).

4.4 NDWI time-series

In order to understand the behaviour of the pond during the seasons and give the correct data on its homogeneity for potential CAL/VAL using, water indices have been extracted. As described in § 3.5, ESA Sentinel-2 imagery has been used to extract NDWI data.
The standard threshold for NDWI to distinguish dried areas from water bodies is typically 0.

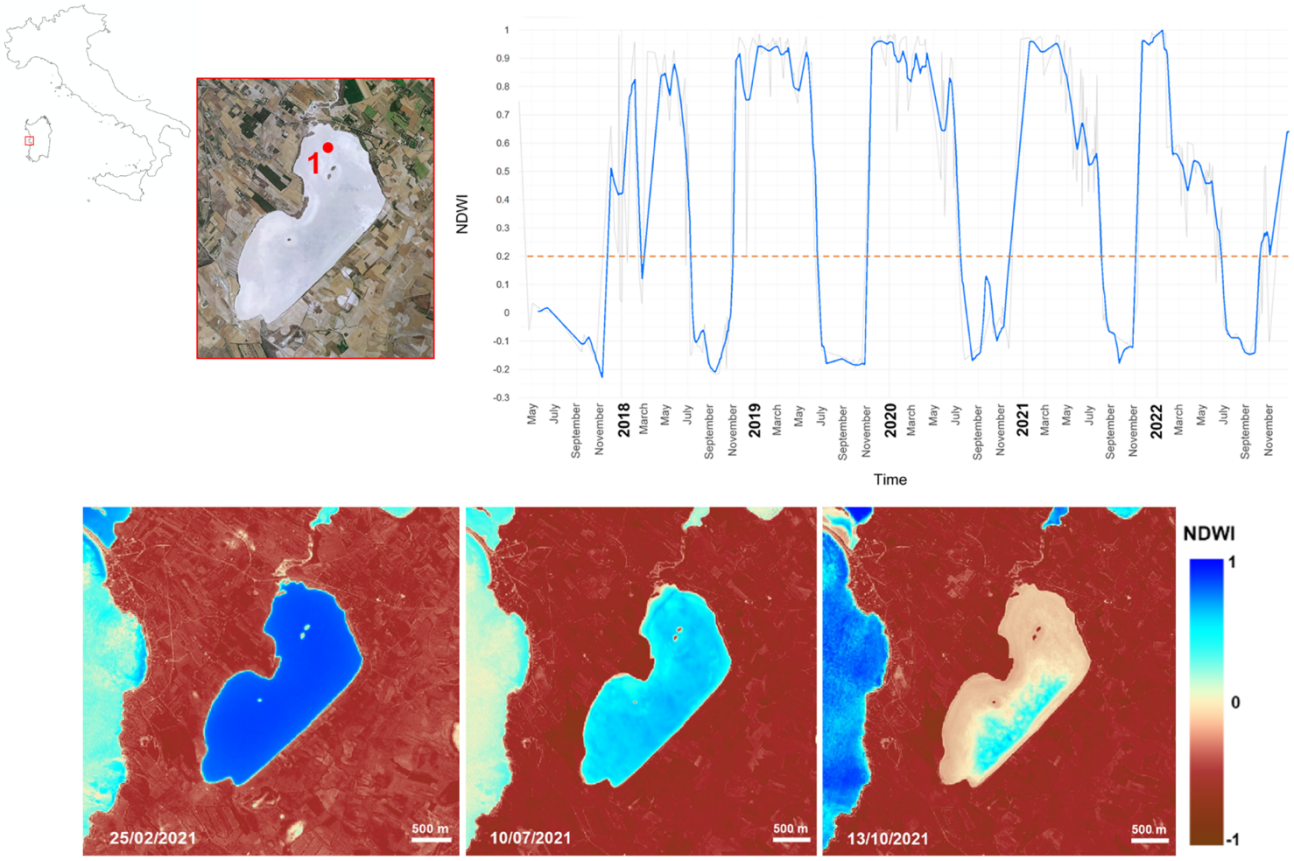

Figure 12. NDWI time-series (top right) relative to the location marked as “1” (in red) shown on the top left. The curve indicates the NDWI trend from March 2017 to December 2022; the periods of drying out are corresponding to the temporal interval where the NDWI dips below the orange dashed line (NDWI threshold of 0.2), indicating no water presence at location 1. Examples of NDWI maps for the dates of February 25, July 10, and October 13, 2021, are shown at the bottom.

However, since even a small amount of moisture on the surface can elevate NDWI values despite the pond being dry, we selected a higher threshold value of 0.20 (Ji L. et al., 2009).
The results from this analysis (Figure 12) show that the duration of drying is largely variable year by year and is extended most likely from July to October. The drying proceeds in north-west/south-east direction: the north-east and north-west areas are the first to dry out, whereas the south-west part rarely dries out completely. Moreover, distinct variations in water presence can be observed over very short intervals, sometimes just a week apart

5. Conclusions

The digital spectral library of surface reflectance covering wavelengths from the VNIR to the SWIR along with sample documentation has been built. The library is dedicated to the salts species outcropping on the SPp. Mineralogical analyses (XRD) on collected samples, reveal a certain compositional homogeneity. The mineralogical analyses have highlighted the presence of the classic minerals belonging to the evaporite series: calcite, dolomite, ankerite, gypsum, and halite. The presence of quartz is not linked to the evaporite series but is probably present as a detrital mineral.
The analysis of the collected spectra shows that sampled sites have similar trend but different absolute value suitable at all for CAL/VAL purposes due to its threshold defined in Berthelot and Santer (2008).
First results of the DTM extracted from UAV LiDAR data confirm that the topography of the surface is flat with elevations ranging from 46.5 m to 46.2 m in the mapped northern part of the pond. The elevation decreases towards eastern bank of the lake, giving the idea of a geological control of this flat area.
The UAV HS data from the northern part of the lake support the findings based on in-situ point field spectrometry and confirm the spectral similarity of the surface material across the sensed area

6. References

Berthelot, B., Santer, R., (2008) Calibration Test Sites Selection and Characterisation CALIB-TN-WP210-001-VEGA (http://calvalportal.ceos.org/c/document_library/)

Clark, R. N., King, T. V. V., and Gorelick, N. S., (1987). "Automatic continuum analysis of reflectance spectra," In Proceedings, Third AIS workshop, 2-4 June, 1987, JPL Publication 87-30, Jet Propulsion Laboratory, Pasadena, California, 138-142.

Clark, R.N., King, T.V.V., Klejwa, M., Swayze, G.A., Vergo, N., 1990. High spectral resolution reflectance spectroscopy of minerals. Journal of Geophysical Research: Solid Earth 95, 12653–12680. https://doi.org/10.1029/JB095iB08p12653

Guarini R. et al., "Prisma Hyperspectral Mission Products," IGARSS 2018 - 2018 IEEE International Geoscience and Remote Sensing Symposium, Valencia, Spain, 2018, pp. 179-182, doi:10.1109/IGARSS.2018.8517785.

Ji L., Zhang L., Wylie B. 2009: Analysis of Dynamic Thresholds for the Normalized Difference Water Index. American Society for Photogrammetry and Remote Sensing, vol. 75, no. 11, Art. no. 11, doi: 10.14358/pers.75.11.1307.

Kaňuk, J., Gallay, M., Eck, C. et al. Technical Report: Unmanned Helicopter Solution for Survey-Grade Lidar and Hyperspectral Mapping. Pure Appl. Geophys. 175, 3357–3373 (2018). https://doi.org/10.1007/s00024-018-1873-2

Kokaly, R.F., Clark, R.N., Swayze, G.A., Livo, K.E., Hoefen, T.M., Pearson, N.C., Wise, R.A., Benzel, W.M., Lowers, H.A., Driscoll, R.L., and Klein, A.J., 2017, USGS Spectral Library Version 7 Data: U.S. Geological Survey data release, https://dx.doi.org/10.5066/F7RR1WDJ.

Melis, M.T.; Pisani, L.; De Waele, J. On the Use of Tri-Stereo Pleiades Images for the Morphometric Measurement of Dolines in the Basaltic Plateau of Azrou (Middle Atlas, Morocco). Remote Sens. 2021, 13, 4087. https://doi.org/10.3390/rs13204087

Musacchio, M.; Silvestri, M.; Romaniello, V.; Casu, M.; Buongiorno, M.F.; Melis, M.T. Comparison of ASI-PRISMA Data, DLR-EnMAP Data, and Field Spectrometer Measurements on “Sale ‘e Porcus”, a Salty Pond (Sardinia, Italy). Remote Sens. 2024, 16, 1092. https://doi.org/10.3390/rs16061092